Catalysis Today 418 (2023) 114122

Contents lists available at ScienceDirect

Catalysis Today

journal homepage: www.elsevier.com/locate/cattod

On the selectivity to ethylene during ethane ODH over M1-based catalysts. A surface and electrochemical study

Agustín de Arriba [a], Ginebra Sánchez [b], Rita Sánchez-Tovar [b], Patricia Concepción [a], Ramón Fernández-Domene [b], Benjamín Solsona [b,*], Jose M. López Nieto [a,*]

[a] Instituto de Tecnología Química, Universitat Politècnica de València-Consejo Superior de Investigaciones Científicas, Avenida de los Naranjos s/n, 46022 Valencia, Spain

[b] Departament dEnginyeria Química, Universitat de València, C/ Dr. Moliner 50, Burjassot, 46100 Valencia, Spain

ARTICLE INFO

Keywords:
Oxidative dehydrogenation of ethane
Electrochemical properties
Mo-V-Te-Nb-O catalyst

ABSTRACT

MoVO, MoVTeO and MoVTeNbO mixed oxides, prepared hydrothermally and heat-treated in N_2 at 400, 500 or 600 °C, are active and selective catalysts in the oxidative dehydrogenation (ODH) of ethane, although their catalytic behaviour strongly depends on the composition and the activation temperature of the material. Thus, the selectivity to ethylene over samples heat-treated at 400 or 600 °C, decreases according to the following trend: MoVTeNb-600 > MoV-400 > MoVTe-600 > MoVTe-400 > MoVTeNb-400 >> MoV-600 (with catalysts heat-treated at 500 °C presenting an intermediate performance). This catalytic performance can be explained to a high extent by the presence of the M1 phase in the best catalysts. Interestingly, the temperature of formation and decomposition of the M1 phase strongly depends on the chemical composition of the catalysts, leading to different trends depending on the heat-treatment temperature. Not only the presence of the M1 phase determines the catalytic performance but also the V^{4+}/V^{5+} ratio in the surface of catalysts. Additionally, a comprehensive brand-new electrochemical characterization of the catalysts has been carried out for MoV-based samples with M1 phase. Accordingly, the best catalytic behaviour in terms of selectivity to ethylene in the ethane ODH was observed in those materials presenting higher charge-transfer resistances at the interfacial active parts and *n*-type semiconductivity with few O-vacancies. Besides, lower current densities obtained in cyclic voltammetries (related to low electrochemical activity) has been associated with higher selectivity in the ODH reaction.

1. Introduction

The oxidative dehydrogenation of ethane (ODHE) is an exothermic process that can operate at relatively low temperatures (300–400 °C) in which catalyst deactivation by coke is minimized due to its in-situ regeneration by the molecular oxygen fed to the reactor [1–6]. Furthermore, this process requires fewer separation units than steam cracking and the number of by-products formed can be reduced to H_2O and carbon oxides (CO_x) [2], although the selectivity to ethylene is the key point to be optimized [1–8]. Thus, from an industrial point of view, ethylene yields between 65 % and 70 % are required to compete with the steam cracking process [7].

Up to date, the most promising catalytic systems for the ODHE are multicomponent mixed metal oxide, i.e. Mo-V-Te-Nb-O catalysts [9,10]. Thus, 75 % ethylene yield can be reached at a reaction temperature of 400 °C, over Mo-V-Te-Nb-O catalysts heat-treated in inert atmosphere at 550–650 °C, but both selectivity to ethylene and yield of ethylene are lower on catalysts with the same composition but heat-treated at 350–500 °C [9]. These catalysts are similar to those developed by Mitsubishi Chemicals researchers for propane (amm)oxidation [10–14].

The outstanding catalytic results of these materials have been related to the presence of the orthorhombic $Te_2M_{20}O_{58}$ (M = Mo, V, Nb) phase (the so-called M1 phase), responsible for the selective activation of C_2-C_4 alkanes [9–26], which is attributed to the presence of isolated active sites on the surface of these catalysts [26]. In addition, the high selectivity to ethylene at high ethane conversion is related to the extremely lower reactivity of ethylene on these catalysts [27].

In the last years, several studies have been conducted in order to optimize the synthesis of the M1 phase, their catalytic behaviour and a greater knowledge of the physical-chemical and structural characteristics [8–30].

Mo-V-Te-O [31–34] and, more recently Mo-V-O [35–38], have been

* Corresponding authors.
E-mail addresses: benjamin.solsona@uv.es (B. Solsona), jmlopez@itq.upv.es (J.M. López Nieto).

https://doi.org/10.1016/j.cattod.2023.114122
Received 30 January 2023; Received in revised form 8 March 2023; Accepted 14 March 2023
Available online 16 March 2023

also proposed as active and relatively selective catalysts in ethane ODH, but also in propane partial oxidation [31,39–42], although the heat-treatment strongly influence the stability of the M1 phase and their catalytic performance. This fact is especially noticeable when comparing the selectivity to ethylene at higher ethane conversion, in which consecutive reactions (and formation of carbon oxides) can be differently favoured [8,27,32–34].

Mo-V-Te-Nb mixed oxide catalysts are known to work through a redox or Mars-Van Krevelen mechanism [26,43]. Interestingly, this type of catalysts based on mixed oxides can work as semiconductors, and surface' oxidation/reduction can be investigated by studying the electrochemical properties of the solid. However, there are very few papers in which electrochemical properties are related to catalytic behaviour. For instance, Wernbacher et al. [44] studied the oxidation of ethane, propane and n-butane and determined the electrical conductivity of the Mo-V-Te-Nb mixed oxides spent catalysts in the reaction by using the Microwave Cavity Perturbation Technique (MCPT). By applying the same technique, Heine et al. [45] investigated the impact of steam on the electronic structure of these catalysts in selective propane oxidation to acrylic acid. Caldararu et al. [46] analysed the changes of the electrical conductivity of a Mo-V-Te-Nb (M2-based) catalyst used in propene oxidation to acrylic acid with the Differential Step Technique (DST).

Nevertheless, in neither of them the technique of Electrochemical Impedance Spectroscopy (EIS) has been applied, which is a powerful non-destructive technique typically used in electrochemistry and from which the resistances of the catalysts can be calculated. Additionally, in these papers, the semiconductor type of the main simple oxides that form the catalysts determine the semiconductor behaviour [44–46], however, it has not been verified by performing capacitance analysis (i.e., Mott-Schottky plots).

Therefore, in this study, we have investigated both the surface nature and the electrochemical properties of MoV-based oxides (M1 phase) and their possible influence on the catalytic performance in the oxidative dehydrogenation of ethane. Moreover, both the catalytic and characterization results have allowed us to find a correlation between the composition and the heat-treatment temperature of the different catalysts with their ability to form the M1 phase.

In this sense, we have synthesized and compared three mixed oxide catalysts presenting high selectivity to ethylene, i.e. Mo-V-O, Mo-V-Te-O and Mo-V-Te-Nb-O, each one of them heat-treated in N_2 at 400, 500 or 600 °C. In order to correlate both composition and structure to the catalytic behaviour, this study was complemented with several characterization techniques such as X ray diffraction (XRD), field emission scanning electron microscopy (FESEM), nitrogen adsorption isotherms and X ray photoelectron spectroscopy (XPS). In addition, a further characterization on the electrochemical properties of these catalysts was also studied by applying the techniques of EIS, Mott-Schottky analysis, and cyclic voltammetries.

2. Experimental

2.1. Catalyst preparation

The catalytic materials were prepared following previously reported methods. Mo-V-Te-Nb-O mixed oxide catalysts were prepared by a hydrothermal method [9,10], from an aqueous solution of ammonium heptamolybdate, vanadyl sulphate, telluric acid and ammonium niobate (V) oxalate hydrate, with a Mo/V/Te/Nb atomic ratio in the synthesis gel of 1/ 0.25/0.17/0.17 at a pH = 2.5.

Mo-V-Te-O catalysts were also prepared hydrothermally, from an aqueous solution of ammonium heptamolybdate, vanadyl sulphate and tellurium dioxide with a Mo/V/Te atomic ratio in the synthesis gel of 1/ 0.37/0.17 at a pH = 2.5 [32,42]. Mo-V-O catalysts were prepared using similar procedures to those previously reported [34,35] with a Mo/V atomic ratio in the synthesis gel of 1/0.37 and at a pH= 3.0.

In all cases, stainless-steel coated Teflon vessels containing the aqueous gels under inert atmosphere were heated at 175 °C for 3 days. The resulting solids were cooled down, washed, filtered and dried at 100 °C for 12 h. Finally, these materials were heat-treated at 400 °C, 500 or 600 °C for 2 h in a N_2 stream. The catalysts will be named as MoV-x, MoVTe-x and MoVTeNbO-x, in which "x" will be the heat-treatment temperature (400, 500 or 600 °C).

2.2. Catalyst characterization

BET specific surface areas were calculated from multi-point N_2 adsorption isotherms at 77 K using a Micromeritics Flowsorb instrument.

X-ray diffraction patterns were collected using a Panalytical X'Pert diffractometer equipped with a graphite monochromator operating at 40 kV and 30 mA, and employing nickel-filtered CuKα radiation (λ = 0.1542 nm).

Thermogravimetric analyses were carried out in a Mettler-Toledo thermobalance (TGA/SDTA 851). To do so, for each analysis, 10 mg of the desired sample was heated under synthetic air (flow of 50 mL min^{-1}) up to 600 °C.

Raman spectra were obtained in an inVia Renishaw spectrometer, equipped with an Olympus microscope. The laser wavelength was 514 nm, generated with a Renishaw HPNIR laser with a power of approximately 15 mW.

Field-emission scanning electron microscopy was performed on a Hitachi S4800 microscope, collecting images at an operation voltage of 5 kV.

X-ray photoelectron spectroscopy (XPS) measurements were performed on a SPECS spectrometer equipped with a Phoibos 150 MCD-9 detector using a monochromatic Al Kα (1486.6 eV) X-ray source. Spectra were recorded using an analyser pass energy of 50 eV, an X-ray power of 100 W, and an operating pressure of 10^{-9} mbar. Spectra treatment was performed using CASA software. In all cases, binding energies were referred to C *1s* at 284.5 eV.

2.3. Electrochemical characterization

Electrochemical Impedance Spectroscopy measurements were performed applying a 0.5 $V_{Ag/AgCl}$ potential using an amplitude of 0.01 V and scanning frequencies from 100 kHz to 0.01 Hz in a 0.1 M Na_2SO_4 electrolyte. Mott-Schottky plots were carried out to evaluate the semiconductor behaviour of the catalysts. These tests were carried out at a 5000 Hz frequency, scanning the potential from 0.5 to − 1 $V_{Ag/AgCl}$ also in a 0.1 M Na_2SO_4 electrolyte. Cyclic voltammetries were performed in a potential range of − 0.1 to 0.6 $V_{Ag/AgCl}$ at 0.01 V/s. In this case, the electrolyte used was a solution of 10 mM $Fe(CN)_6K_4$ with 0.1 M Na_2SO_4. For every study, a three-electrode electrochemical cell was used. The catalyst was the working electrode (deposited on FTO) connected to the potentiostat. A platinum tip was placed as the counter electrode and Ag/AgCl (3 M KCl) was used as the reference electrode. An area of 0.5 cm^2 of the catalysts was exposed to the electrolyte.

2.4. Catalytic tests

The catalytic experiments were carried out in a fixed-bed quartz tubular reactor working at atmospheric pressure and in a 350–425 °C temperature range. The flow rate (25–100 mL min^{-1}) and the amount of catalyst (0.05–1.0 g; 0.25–0.50 mm particle size) were varied in order to achieve different ethane conversions. Silicon carbide was added to maintain a bed size of ca. 3 cm^3 in order to avoid heat-transfer problems. The reaction mixture (ethane/oxygen/helium) was fed with a molar ratio of 5/5/90. Reactants and reaction products were analysed by an online gas chromatograph (Agilent 7890A) equipped with two packed columns [9,10]: (i) Porapak Q (3 m) to separate carbon dioxide, water, hydrocarbons and acids; (ii) molecular sieve 5Å (3 m) to separate O_2 and CO.

3. Results and discussion

3.1. Characterization of catalysts

The physicochemical characteristics of mixed oxides, i.e., Mo-V-O, Mo-V-Te-O and Mo-V-Te-Nb-O catalysts, heat-treated at 400, 500 or 600 °C in an inert atmosphere, are shown in Table 1.

Fig. 1 shows, separately, the XRD patterns of as-synthesized materials and those catalysts heat-treated at different activation temperatures. For both **MoV-as** and **MoVTe-as,** it can be seen the single-phase orthorhombic M1-type structure (ICSD no. 55097) [44,45], whereas the **MoVTeNb-as** presents a XRD pattern of a pseudocrystalline phase, with strong anisotropic peak at ca. 2θ = 23.0, suggesting a preferential crystallization along the C-axis direction [47].

The XRD patterns of heat-treated samples indicate an opposite trend between MoVO-series and those observed for MoVTeNbO-series, with MoVTeO-series presenting M1 phase in all range of activation temperatures. Thus, both intensity and definition of the diffraction peaks in the **MoV-400** sample suggests the almost only presence of orthorhombic M1 phase with the highest degree of crystallinity. Similarly, M1 phase is also observed for the **MoV-500** sample. However, tetragonal $(Mo_{0.93}V_{0.07})_5O_{14}$ phase, with diffraction peaks at 2θ = 22.3, 25.0, 31.6 and 33.7° [35], is mainly observed for sample **MoV-600**, as a consequence of the degradation of the orthorhombic phase.

In the case of MoVTeNb-series, the XRD patterns indicate the prevalence of the pseudocrystalline phase until activation temperatures beyond 500 °C. However, for the MoVTeNb catalyst heat-treated at 600 °C, the M1 phase is almost the only phase detected. In fact, for this catalyst, characteristic diffraction peaks at 2θ = 6.7°, 7.9°, 9.0°, 10.8°, 23.0° and 27.3° (ICSD no. 55097) [44,47] with a partial arrangement of the atoms along the C-axis, as seen for the only sharp peak at 2θ = 23.0°, have been observed.

Conversely to MoV-samples, when heat-treated at 600 °C, the quaternary **MoVTeNb-600** catalyst is the one with the highest definition and intensity in the diffraction peaks. Then, low heat-treatment temperatures are required to avoid the M1 decomposition in MoV-catalysts (lower than 500 °C), whereas higher temperatures (over 500 °C) are required for the formation of the M1 phase in MoVTeNb-based catalysts. Furthermore, the inverse intensity relationship between the two most characteristic diffraction peaks (i.e., 23.0° and 27.3°) in **MoV-400** and **MoVTeNb-600** samples suggests a marked change in the morphology of the oxides, which has been studied and it is discussed below. In addition, it must be noted that the ternary Mo-V-Te catalysts, both at 400, 500 and 600 °C, present a well-defined pattern of the M1 structure, with intermediate intensity and peak relationships.

Table 1
Characteristics of the MoV(Te,Nb)O catalysts.

Catalyst	Mo/V/Te/Nb at. composition[1]	Mo/V/Te/Nb at. XPS composition [1]	V^{+4}/V^{+5} ratio (XPS)	Surface area (m^2 g^{-1})
MoV-400	1/0.37/0/0	1/0.18/0/0	75/25	35.2
MoV-500	1/0.37/0/0	1/0.16/0/0	50/50	21.4
MoV-600	1/0.34/0/0	1/0.13/0/0	34/66	7.2
MoVTe-400	1/0.37/0.13/0	1/0.08/0.10/0	44/56	20.3
MoVTe-500	1/0.38/0.10/0	1/0.22/0.03/0	62/38	17.6
MoVTe-600	1/0.46/0.08/0	1/0.17/0.05/0	66/34	7.9
MoVTeNb-400	1/0.23/0.21/0.22	1/0.14/0.28/0.27	40/60	55.1
MoVTeNb-500	1/0.23/0.21/0.22	nd	nd	35.0
MoVTeNb-600	1/0.22/0.26/0.23	1/0.14/0.40/0.28	85/15	17.0

1) Catalyst after activation done by EDX.

Further characterization results, such as Raman spectra, are shown in the Supporting Information (Fig. S1). In all cases, the spectra obtained present the main features of the M1 phase [42,48], i.e., an intense peak centred at ca. 874 cm^{-1}, with shoulders at higher and lower wavenumber. Shoulder in the 770–880 cm^{-1} region is attributed to asymmetric Me-O-Me bridge stretching modes, whereas the symmetric ones can be seen at 470 cm^{-1}. In addition, the shoulder at 970–980 cm^{-1} corresponds to Mo═O and V═O terminal stretching vibrations. In the case of **MoVTeNb-400** (although not presenting a more defined principal peak due to its non-crystalline shape) and **MoVTeNb-600** samples, weak shoulders at 650 and 820 cm^{-1} are ascribed to the formation of Nb-O-Nb bonds, where isolated NbO_6 octahedra give rise to a signal at ca. 907 cm^{-1} [49].

In order to study the stability of the three catalysts' composition, we performed thermogravimetric studies on as-synthesized samples (i.e., **MoV-as**, **MoVTe-as** and **MoVTeNb-as**) and the experimental results are shown in Fig. S2. In this case, the TG patterns of **MoV-as**, **MoVTe-as** and **MoVTeNb-as** materials seem to have a quite similar tendency although with different slopes. In all cases, first weight losses until 150 °C are associated with H_2O molecules adsorbed. Second drops in mass appear at around 250 °C, in this case attributed to NH_4^+ and maybe also H_2O occluded into the micropores of the structure. Then, from ca. 350 °C, a small but constant weight gain is observed for both **MoV-as** and **MoVTeNb-as** catalysts, or a sudden gain can be seen for **MoVTe-as** at 470 °C, as a consequence of oxidation of the material.

Fig. 2 shows some representative FE-SEM images of the different catalysts activated at 400 or 600 °C. Fig. 2a displays the FE-SEM image of the **MoV-400** catalyst. There, elongated needles (typical of M1 phase [24]) with high crystallinity can be elucidated. These needles are, in some regions, connected to others. Nevertheless, for the **MoV-500** catalyst (Fig. 2b), the structure undergoes a notable depletion in its crystallinity, exhibiting in some cases an amorphous shape (there is almost no elongated needle structures) that, in fact, perfectly correlates with XRD results (seen in Fig. 1a), where a deep decrease in the relative intensity of the diffraction peaks is shown for **MoV-500**. This fact suggests that the M1 phase begins to decompose in MoV-series when activation temperature increases above 400 °C. For the **MoVTe-400** and **MoVTe-600** catalysts (Fig. 2c and d, respectively) a needle structure, indicative of the M1 phase, is also observed, regardless the calcination temperature. The thickness of the needles is roughly 0.5 μm and different lengths are obtained, depending on the agglomeration of the needles, in some cases, reaching more than 9 μm. In addition, Fig. 2e and h how also that the morphology of the MoVTeNbO catalysts changes with the activation temperature, especially for the catalysts heat-treated at 400 °C, where particles with somehow a globular shape are presented. The morphology of sample **MoVTeNb-600** is similar to those observed for samples **MoV-400** or MoVTe-series, but more compact and with short rods/cylinders (see Fig. 2h), consistent with the M1 phase [34]. These results are in agreement with XRD data, since M1 phase is not formed in the **MoVTeNb-400** catalyst.

In order to explain the catalytic behaviour of these catalysts, several factors rather than the presence of the M1 phase must be considered as well, since not all the catalysts presenting the M1 phase perform equal. Then, according to FESEM and XRD studies, among the catalysts with well-formed M1 phase and high degree of crystallinity, the most selective sample is the one that possesses the most compact needles (**MoVTeNb-600** catalyst). A possible explanation lies on the fact that the active sites of the M1 phase are located on the bases of the cylindrical structures that form this catalyst (001 basal face of the needle) [50,51].

Moreover, those differences observed in the morphology of the catalysts treated at 400, 500 or 600 °C can lead to dissimilar textural properties. In that sense, N_2 adsorption isotherms were carried out, and the results for surface area and micropore volume are shown in Table 1 and Fig. S3. Interestingly, surface area depends strongly on both the composition and the activation temperature of the catalyst [52]. For instance, among the catalysts heat-treated at 400 °C, the sample with the

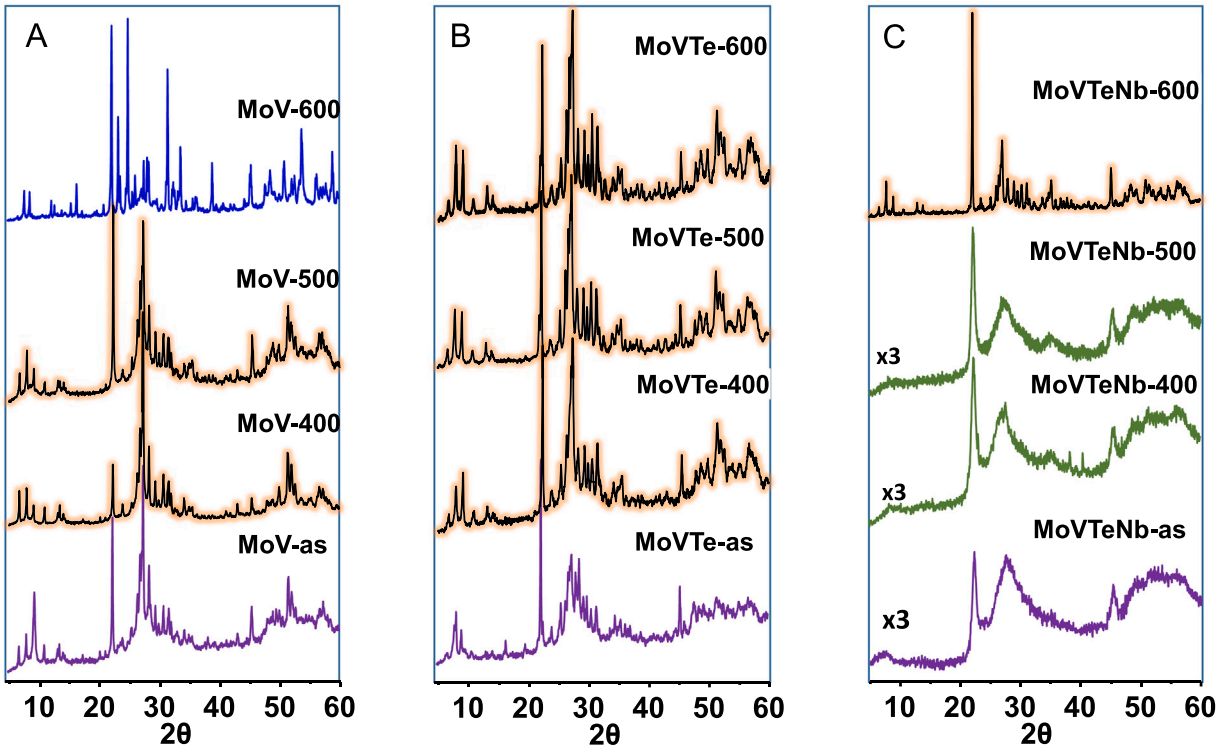

Fig. 1. XRD patterns of **MoV-** (A), **MoVTe-** (B) and **MoVTeNb**-series (C): as-synthesized samples, and catalysts heat-treated at 400, 500 or 600 °C in a N_2 atmosphere. Characteristics of catalysts in Table 1.

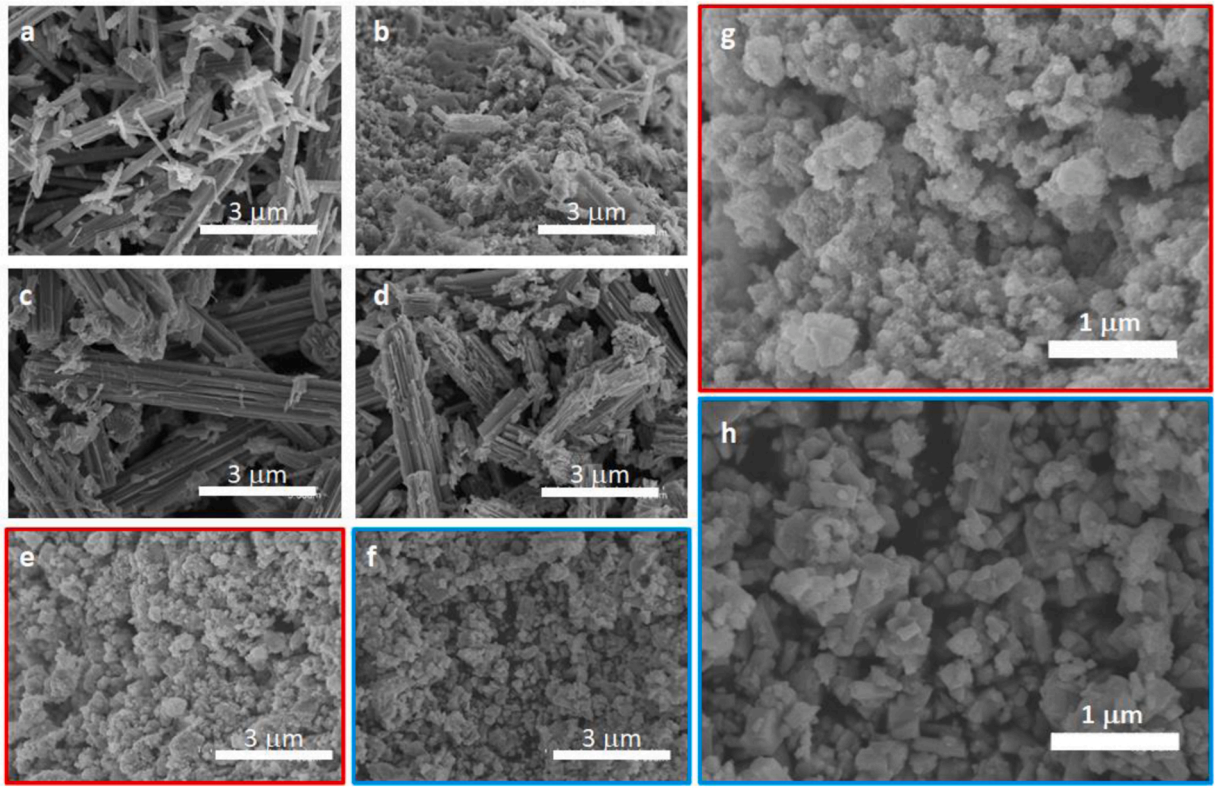

Fig. 2. FESEM images of the different catalysts: **MoV-400** (a), **MoV-500** (b), **MoVTe-400** (c), **MoVTe-600** (d), **MoVTeNb-400** (e) and **MoVTeNb-600** (f). Images (g) and (h) are the magnification of images (e) and (f), respectively.

highest surface area value is **MoVTeNb-400** (ca. 55 m^2 g^{-1}). However, the surface area decreases when increasing activation temperature, up to 35 m^2 g^{-1} (**MoVTeNb-500**) or 17 m^2 g^{-1} (**MoVTeNb-600**). In a similar way, for binary and ternary M1 catalysts, a higher surface area of the sample activated at 400 and 500 °C compared to the 600 °C-treated counterpart has been observed: ca. 35, 21 and 7 m^2 g^{-1}, for MoV-series, respectively, and ca. 20, 18 and 8 m^2 g^{-1}, for MoVTe-series, respectively. Accordingly, as a general trend for the three families of catalysts, the higher the thermal activation the lower the surface area, regardless of the chemical composition.

3.2. Catalytic results for ethane ODH

Catalysts with different chemical composition (Mo-V-O, Mo-V-Te-O and Mo-V-Te-Nb-O) and different thermal activation temperatures were tested in the ODH of ethane (Table S1) and results are comparatively shown in Table 2. Both chemical composition and activation temperature lead to huge differences among the different samples. Nevertheless, it must be stated that all the samples not presenting the M1 phase (i.e., samples **MoV-600**, **MoVTeNb-400** or **MoVTeNb-500**) have the worst catalytic properties in terms of catalytic activity (sample **MoV-600)** and/or selectivity to ethylene (samples **MoVTeNb-400** or **MoVTeNb-500**).

Especially notorious is the case of the bimetallic MoV-based catalysts, in which big differences have been observed in activity and selectivity to ethylene. This behavior can be related to the absence of the M1 phase in the **MoV-600** catalyst (decomposed into $(MoV)_5O_{14}$-based phase), as observed by XRD (Fig. 1A). For the MoVTe-based catalysts, a more severe thermal activation implied a decrease in the surface area, however, it also led to a higher selectivity to ethylene (Table 2), with the corresponding decrease in the catalyst's activity, as in the case of MoVTeNb catalysts (Table 2). It must be noted that, unlike for MoV- and MoVTeNb-series, samples of MoVTe-series presented the M1 structure for the three temperatures studied and, therefore, changes in the surface area, as well as the micropore volume, can modify the rate for ethane conversion when considering number of V-sites and surface area (Table 2).

Table 2
Catalytic parameters of MoV-containing catalysts in the oxidative dehydrogenation of ethane to ethylene.[a]

Catalyst	Reaction rate[b]	Areal rate[c]	Rate per active site[d]	Rate per active site and area[e]	Selectivity to ethylene (%)[f]
MoV-400	15.1	0.43	142.5	4.05	75
MoV-500	7.8	0.36	73.6	3.44	66
MoV-600	0.34	0.05	3.2	0.45	nd[g]
MoVTe-400	2.8	0.15	29.5	1.45	65
MoVTe-500	3.3	0.19	33.2	1.89	78
MoVTe-600	3.4	0.27	29.3	3.71	88
MoVTeNb-400	2.4	0.04	46.2	0.84	56
MoVTeNb-500	2.1	0.06	40.4	1.15	65
MoVTeNb-600	5.2	0.31	109.5	6.44	95

[a)] Conditions in the Experimental section, at 390 °C and C_2/O_2/He: 5/5/90 molar ratio; [b)] Reaction rate of ethane conversion (in 10^3 mol_{C2H6} g_{cat}^{-1} h^{-1}), calculated at ethane conversion below 10 %; [c)] Areal rate of ethane conversion (in $mmol_{C2H6}$ m^{-2} h^{-1}), calculated at ethane conversion below 10 %; [d)] Reaction rate of ethane conversion per active site (in 10^3 mol_{C2H6} g_V^{-1} h^{-1}), calculated at ethane conversions below 10 %; [e)] Reaction rate of ethane conversion per active site and area, in 10^3 mol_{C2H6} (100 %V)$^{-1}$ m^{-2} h^{-1}, calculated at ethane conversions below 10 %; [f)] Selectivity to ethylene for an ethane conversion of 50 %; [g)] due to the poor activity, conversions higher than 25 % have not been reached.

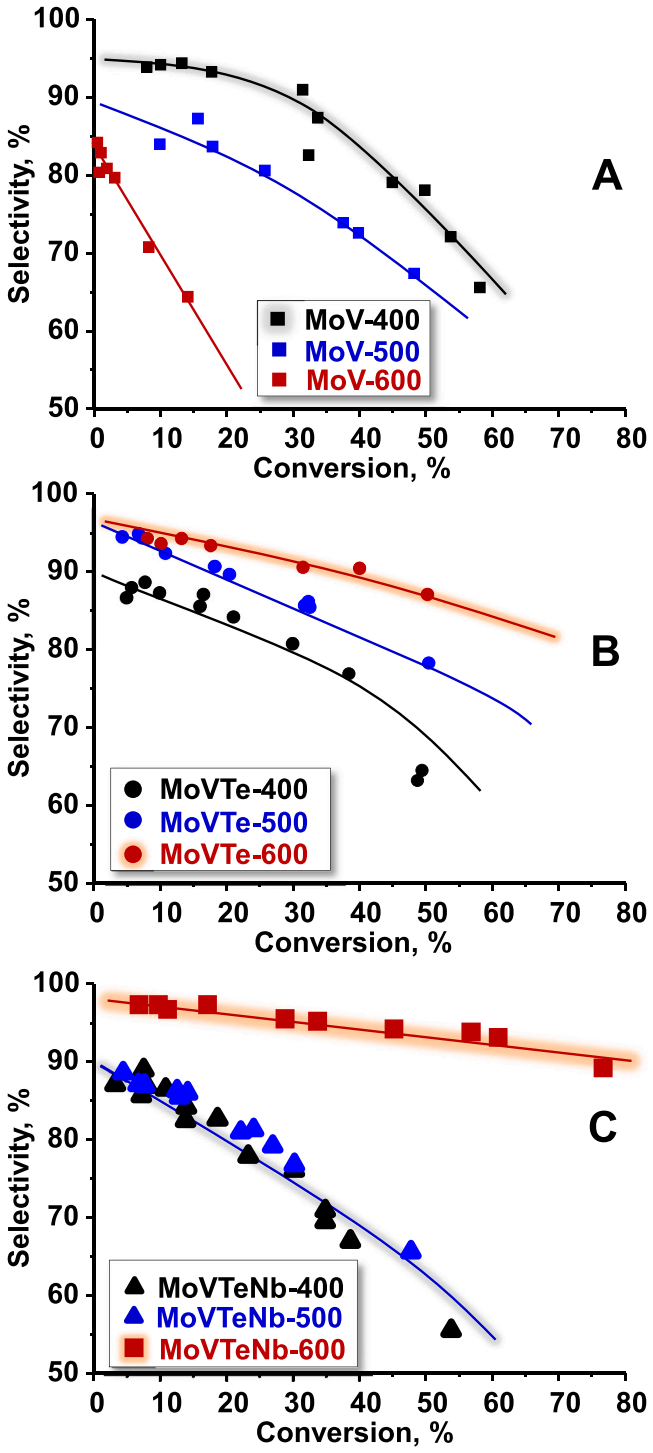

Fig. 3. Variation of the selectivity to ethylene with the ethane conversion during the ethane ODH at 390 °C. A) MoV-series; B) MoVTe-series; C) MoVTeNb-series. Reaction conditions in text. Characteristics of catalysts in Table 1.

Fig. 3 presents the variation of the selectivity to ethylene with ethane conversion at 390 °C for all the studied catalysts. In the case of the binary MoV-series (Fig. 3A), the best catalytic results were observed for the catalyst with the lowest activation temperature (i.e., **MoV-400**), whereas the selectivity to ethylene decreased with the activation temperature.

Especially notorious is the drop in the selectivity obtained in the **MoV-600** sample, in which selectivity values are up to 30 % lower than

those observed for **MoV-400**, in addition to a completely different trend in the activity, probably due to the partial transformation of the M1 phase into non-catalytic crystalline phases reported previously [25,53]. In any case, **MoV-500** showed selectivity values ca. 10 % lower than its 400 °C-treated counterpart, maintaining said differences at high values of ethane conversion (for instance, 75 % selectivity to ethylene for **MoV-400** versus 66 % for **MoV-500** at 50 % conversion).

On the contrary, inverse results were obtained in the case of the ternary Mo-V-Te-O catalysts (Fig. 3B). In this case, the selectivity to ethylene increased with the temperature of the thermal activation, with a maximum for the catalyst treated at 600 °C (**MoVTe-600**), followed by **MoVTe-500** and then **MoVTe-400**, although the biggest differences are appreciable at higher ethane conversions (<30 %).

Moreover, if compared with the binary catalysts, the **MoVTe-400** sample presents lower selectivity values than those of the **MoV-400**, whereas **MoVTe-600** exhibits fairly higher values than the latter, and obviously a more evident difference than the partially M1 structure collapsed **MoV-600** catalyst.

The results for MoVTeNb-series are presented in Fig. 3C. In this case, and as previously reported for propane oxidation [42], the selectivity to ethylene is tightly related to the activation temperature of the catalysts, since no perfectly crystalline M1 phase is formed for activation temperatures below 550 °C. Therefore, as observed in that figure, extremely high differences in ethylene selectivity can be discerned between the catalysts **MoVTeNb-400 or MoVTeNb-500** (both pseudo-crystalline phases) and **MoVTeNb-600** (pure M1 phase). In this series, samples calcined at 400 and 500 °C presented a practically identical selectivity to ethylene, with a strong decline with conversion, in contrast to what it is seen for the catalyst calcined at 600 °C, presenting an excellent selectivity to ethylene beyond 90 % for all the conversion values studied. Moreover, the **MoVTeNb-600** sample is the one that presented the highest selectivity to ethylene among all the series, with very low ethylene combustion (selectivity to ethylene up to 95 % at 70 % of ethane conversion) (Fig. S4). Accordingly, the significant decrease in C_2H_4 selectivity with increasing conversion on MoVTeNbO catalysts heat-treated at 400 or 500 °C can be related to the absence of M1 phase [53].

Furthermore, by looking at the catalytic results, it can be stated that not only the selectivity to ethylene depends on the thermal treatment, also the catalytic activity of the samples studied is related to both the composition and the activation temperature. Then, Fig. 4A, shows that **MoV-400** catalyst is remarkably more active (normalized per mass) than **MoVTe-400** and **MoVTeNb-400** catalysts. However, comparing to catalysts heat-treated at 600 °C, the highest activity is obtained by the **MoVTeNb-600** catalyst. Overall, the highest rate per mass of catalyst corresponds to the MoVTeNbO catalyst activated at 600 °C (**MoVTeNb-600)**, slightly higher than the binary MoVO sample activated at 400 °C (**MoV-400)**.

Conversely, by jointly normalizing per surface area and per V site (Fig. 4B), for the MoV-catalysts, the activity increases when decreasing the heat-treatment temperature, the same as if normalized per mass. Moreover, the same trend as observed in Fig. 4A is displayed for MoVTeNb-based catalysts applying this new normalization, in where, reaction rate increases when increasing the heat-treatment temperature (Fig. 4B). Lastly, in the case of MoVTe-catalysts, the reaction rate per active site and surface area is very similar regardless of the activation temperature. Nevertheless, differences in terms of activity are more notorious by applying the normalization used in Fig. 4B, with the **MoVTeNb-600** still being the most active catalyst.

Moreover, apart from ethylene, the other reaction products that have been obtained are mainly CO and CO_2. In the binary MoVO catalysts, acetic acid has been also detected, although with a selectivity lower than 2 %. For the ternary and quaternary catalysts, the presence of acetic acid has been only observed as traces. For all catalysts, the selectivity to ethylene at low conversions is high. Then, by decreasing the space velocity, the ethane conversion can be increased. Unfortunately, at higher conversions the selectivity to ethylene decreases, whereas the selectivity to carbon oxides increases, especially in the case of the binary MoV catalysts. This means that, initially, ethane is in all cases mainly transformed into ethylene but with some CO_x ($CO+CO_2$) formation and, at some point, some of the ethylene formed also decomposes into carbon oxides. Nevertheless, among the carbon oxides, the formation of CO is predominant in the ethylene decomposition for all the catalysts regardless of the chemical composition and the activation temperature.

All in all, the catalysts that presented the best catalytic performance in terms of activity and selectivity to ethylene among the series were: **MoV-400**, **MoVTe-600** and **MoVTeNb-600**. These results suggest a positive effect of the activation temperature only when Te^{4+}, and both Te^{4+} and Nb^{5+} species are incorporated into the M1 structure.

3.3. *Characterization of the surface of catalysts*

Although the selection of the proper crystalline phase is indispensable [51–54], the surface of the M1 structure is the one directly involved in the activation of alkanes in selective oxidation reactions. Accordingly, a surface study by XPS has been undertaken and the results are comparatively shown in Fig. 5 and Table 1.

The XPS Mo *3d* core level spectra for catalysts heat-treated at 400 or

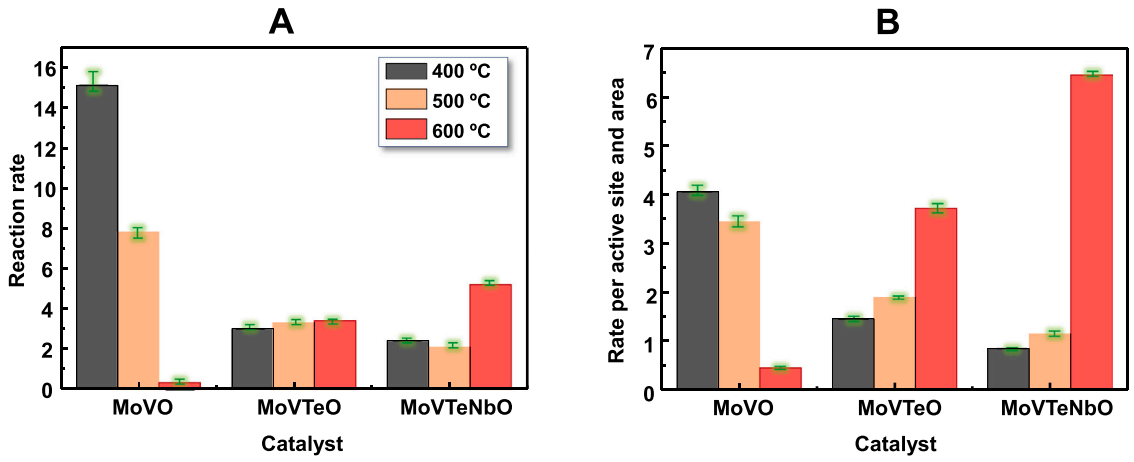

Fig. 4. Reaction rate of ethane conversion (A) and Reaction rate of ethane conversion per site and per area (B) of MoVO-, MoVTeO- and MoVTeNbO-series, heat-treated at 400, 500 or 600 °C, during the ethane ODH. Reaction conditions: 390 °C and C_2/O_2/He: 5/5/90 molar ratio. Reaction rate as 10^3 mol_{C2H6} g_{cat}^{-1} h^{-1} at ethane conversions below 10 %. Reaction rate per active site and area as 10^3 mol_{C2H6} (100 %V)$^{-1}$ m^{-2} h^{-1} at ethane conversions below 10 %. Green bars correspond to error bars.

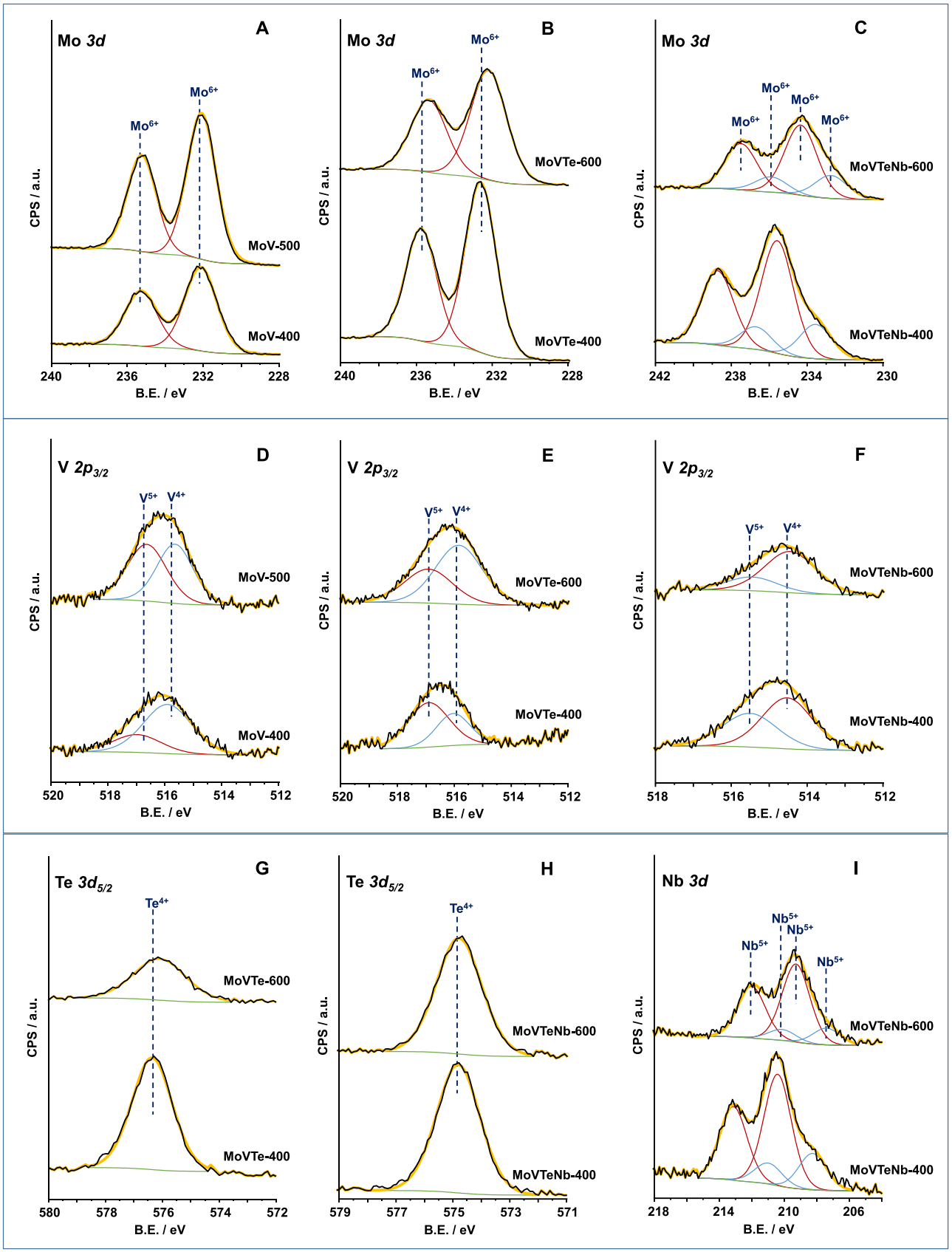

Fig. 5. XPS spectra of catalysts heat-treated at 400 °C or 600 °C: Mo *3d* XPS spectra (A–C); V $2p_{3/2}$ XPS spectra (D-F); Te $3d_{5/2}$ XPS spectra (G, H); and Nb *3d* XPS spectra (I).

600 °C are shown in Fig. 5A-C. Spectra for the MoVO and MoVTeO catalysts are very similar to each other and indicate that molybdenum is totally oxidized on the surface of the catalysts, only presenting the +6 oxidation state (Mo^{6+} signals presenting a doublet at 235.7 and 232.5 eV, corresponding to the Mo $3d_{5/2}$ and Mo $3d_{3/2}$ components, respectively, with a spin orbit split of ca. 3.15 eV) [24,55,56]. On the other hand, for MoVTeNbO catalysts, a second doublet related to differential charging within the measurement is observed, probably due to the inclusion of the Nb^{5+} cations in the centre of the pentagonal units of the structure as will be indicated latter.

The XPS V $2p_{3/2}$ core level spectra of all the catalysts (Fig. 5D–F) are formed by the contribution of two components with binding energies around 517.5 eV and 516.5 eV, which have been related in the literature to the presence of the V^{5+} and V^{4+} oxidation states, respectively [24,55,57,58]. However, this ratio presents rather different values depending on both the composition of catalysts and the activation temperature.

Fig. 5G and H show the Te $3d_{5/2}$ core level spectra of the ternary and quaternary catalysts. In all of them, it is clearly shown a unique tellurium signal at 576.3 eV of binding energy, corresponding to Te^{4+} species [24,55,58], although with slight shifts between them, which are likely related to the different environments.

Finally, the Nb *3d* XPS spectra of the Mo-V-Te-Nb-O catalysts showed mainly the presence of Nb^{5+} (at 210.4 and 213.1 eV for Nb $3d_{5/2}$ and Nb $3d_{3/2}$ components, respectively) (Fig. 5I) [24,55,58]. Additionally, a second doublet at ca. 208.2 and 210.9 eV can be also observed, likely linked to differential charging within the measurement.

According to the XPS results, we have not been able to find a relationship between the oxidation state of molybdenum and its catalytic properties. In this sense, quaternary catalysts are the only ones that could present a certain proportion of Mo^{5+}, very similar in both cases (14–15 %), nevertheless that signals are most likely due to differential charging rather than to a real Mo^{5+} percentage in the sample. However, the catalytic performance is very different; in fact, they present the highest and the lowest selectivity to ethylene of the whole series.

Conversely, the surface study of the V-species seems to be able to predict the performance of the catalysts. Then, it has been observed that the higher the proportion of V^{4+} species, the higher is the selectivity to ethylene. This fact is reflected in Fig. 6, where a clear correlation is shown between the total amount of V^{4+} species determined by XPS and the selectivity to ethylene. This is especially notable as this relationship takes place regardless of the composition of the catalyst and the activation temperature. As vanadium is reported to be the active site in this type of catalysts [9–27], it can explain the lack of trend observed with molybdenum.

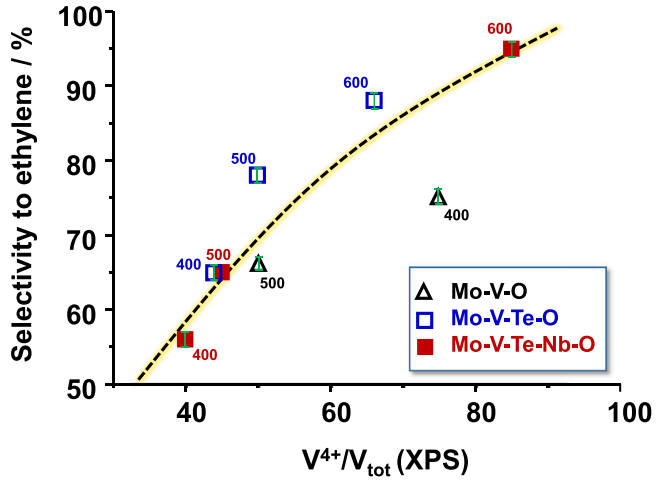

Fig. 6. Variation of the selectivity to ethylene (at an ethane conversion of 50 %, see Table 2) with the V^{4+}/V_{total} determined by XPS (see Table 3) of MoV-, MoVTe- and MoVTeNb-series, heat-treated in N_2 at 400, 500 or 600 °C. Green bars correspond to error bars.

In this way, a catalyst with a more compact morphology (as in the case of the **MoVTeNb-600** sample) seems to contain the vanadium atoms (V^{4+} species, precisely) in a more favourable environment for the selective activation of ethane.

It is well-accepted that the selective oxidative activation of ethane or propane is carried out on V^{5+}-sites ($V^{5+}{=}O \leftrightarrow {}^{4+}V^{\bullet}{-}O^{\bullet}$) [16,17,26,43,50,54], by abstracting a methylene hydrogen from the alkane. In this way, it has been proposed the importance of nucleophilic bridging oxygen atoms between reduced and oxidized metal centres during the partial oxidation of alkanes [26,50], specifically the bridging oxygen atoms in V^{5+}-O-Me units (Me= $Mo^{6+/5+}$ or $V^{5+/4+}$) in which the nucleophilicity of the oxygen bounded to V^{4+} should be higher than that bounded to V^{5+} [59,60]. However, an excess of lattice oxygen on the catalyst surface could also favour consecutive reactions of desorbed olefins [27].

According to the site isolation hypothesis proposed by Grasselli [25,50,61,62]], a partially reduced surface (with the appearance of V^{4+} sites) could have a positive effect in the selectivity to ethylene by decreasing ethylene deep oxidation, which is in agreement with the relationship observed between selectivity to ethylene and the surface V^{4+}/V_{tot} ratio. The low specificity of isolated V^{4+} species to ethylene transformation (probably in V–O–Mo pairs in the heptagonal channels) can be a key factor in the high selectivity to ethylene [27].

For this reason, and in addition to the isolation of active sites in the terminal [001] plane [16,17,26,43,50,54,61,62], the optimization of V^{4+}/V^{5+} ratio on the catalyst surface, could prevent undesirable consecutive reactions improving the selectivity to ethylene at high ethane conversion as observed in our catalysts. Accordingly, some V^{5+} would be necessary for the alkane oxidation but in relatively low proportions (in agreement with the relationship observed between selectivity to ethylene and the surface V^{4+}/V ratio).

3.4. Electrochemical characterization

As the oxidation state of the active species and the transfer of oxygen from the lattice to the surface with its corresponding electron transfer are involved in the selective ethylene formation, we have studied the electronic (semiconducting) nature of the catalysts and the electrochemical properties of their interfaces.

First, electrochemical impedance spectroscopy (EIS) measurements were performed in order to study the resistance of the different samples to charge-transfer processes. Then, Fig. 7 shows the Nyquist (Fig. 7a) and Bode-module (Fig. 7b) plots for the binary (MoV-series), ternary (MoVTe-series) and quaternary (MoVTeNb-series) oxides, heat-treated in the 400–600 °C temperature range.

It can be seen that, regardless of the sample, all Nyquist plots display two semicircles. These semicircles correspond with two regions with different slopes in Bode-module plots. The first semicircle (obtained at high and intermediate frequencies) can be associated with the charge-transfer response of the oxide/electrolyte interface [63,64], hence providing information on the active surface of the catalysts.

The second semicircle can be attributed to the catalyst bulk [64,65], that is, the part of the oxide which is not active from a catalytic point of view. In general, the higher the semicircle amplitude, the higher the impedance of the electrochemical process related to it. Observing Fig. 7a, the catalyst with the largest semicircles is **MoVTeNb-600**, which means that this quaternary oxide has the highest impedance. Binary and ternary oxides provide significantly lower impedance values for both semicircles.

The morphology of Nyquist and Bode-module plots suggests that an electrical equivalent circuit with two parallel R-C time constants should be used to simulate the EIS results, as shown in Fig. 7c. In this circuit, constant phase elements (CPEs) have been used instead of capacitors to account for the non-ideality of the system. From this circuit, the resistance R_1 has been quantified, which is the charge-transfer resistance at

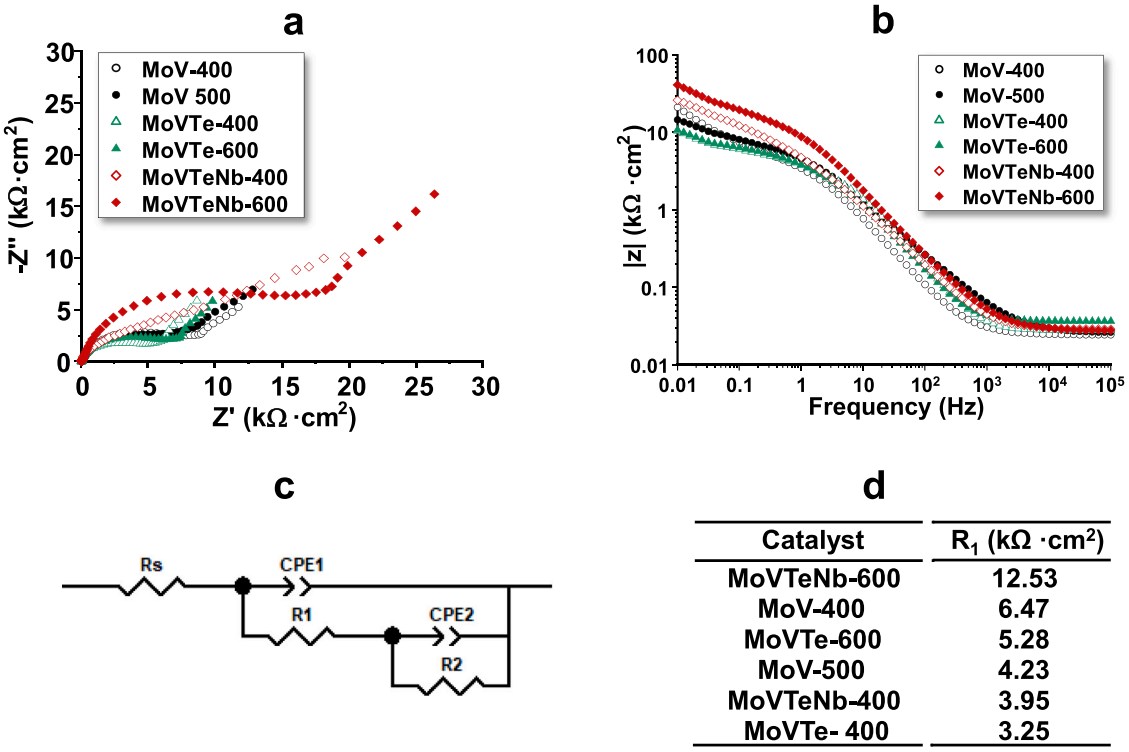

d

Catalyst	R_1 (kΩ·cm²)
MoVTeNb-600	12.53
MoV-400	6.47
MoVTe-600	5.28
MoV-500	4.23
MoVTeNb-400	3.95
MoVTe- 400	3.25

Fig. 7. Nyquist (a) and Bode-module plots (b) for some representative catalysts showing M1 structure. Equivalent circuit used to fit EIS data (c). Charge-transfer resistance (R_1) at the active parts of the catalysts/electrolyte interface (d).

the active parts of the catalysts/electrolyte interface (Fig. 7d). R_1 values are considerably higher for the **MoVTeNb-600** catalyst.

In Fig. S5 the cyclic voltammetries, first and last (10th) cycle, obtained for the different studied catalysts are presented. There, two peaks can be ascertained: one cathodic peak at ~0.18 $V_{Ag/AgCl}$ and another anodic peak at ~0.30 $V_{Ag/AgCl}$, associated with the typical electrochemical response of the Ferri/Ferro redox pair. Thus, both cyclic voltammetries are very similar for each catalyst, confirming the stability of the samples in every composition.

Interestingly, while a correlation between resistance to charge-transfer at the catalysts active parts (R_1) and their selectivity towards ethylene is found and plotted in Fig. 8A, a completely different trend is observed when it comes to the influence of the anodic current density values referred to the selectivity to ethylene of the catalysts (Fig. 8B). Then, as shown in Fig. 8A, higher R_1 values result in higher selectivity to ethylene in the ethane ODH. Therefore, the high charge-transfer resistance at the interfacial active parts (surface) of the catalysts, as suggested from the differential charging observed by XPS in sample **MoVTeNb-600**, is related to better selectivity to ethylene during the ethane ODH.

Conversely, Fig. 8B shows an inverse correlation between the anodic current density values of the catalysts and the selectivity to ethylene. The explanation for this trend could lay on the fact that higher current densities are generally attributed to an enhanced electrochemical activity of the catalysts, thus favouring total oxidation reactions, this is, the transformation of ethane (or ethylene) into carbon oxides. According to this relationship (Fig. 8B), catalysts with lower current densities are desired to improve the selectivity to ethylene during the ethane ODH in order to reduce the deep oxidation of ethane and ethylene into carbon oxides.

Additionally, the variation of the selectivity to ethylene with the anodic current density (Fig. 8B) or with the V^{4+} concentration on the catalyst surface (Fig. 6) follows opposite trends. In fact, this might be attributed to the lower number of electrophilic oxygens (which are responsible for non-selective oxidation reactions) in the catalysts with higher V^{4+} surface content (less oxidized active surface), which results in an enhancement in the selectivity to ethylene. On the other hand, higher current densities could be related with a higher proportion of electrophilic oxygens, thus, decreasing the selectivity to ethylene.

Furthermore, to study the influence of the semiconducting properties of the different oxides with their catalytic performance, Mott-Schottky analyses have been also performed. Fig. 9 shows the Mott-Schottky plots for the catalysts studied.

In the case of the binary MoVO oxides heat-treated at 400 °C or 500 °C two clear linear regions can be seen. The linear region with positive slope (from −0.6 V to aprox. 0.1 V) indicates an *n*-type semiconducting behaviour, while the negative slope at higher potentials is characteristic of *p*-type semiconductivity. For comparison, Fig. S6 (Supporting Information) also shows the Mott-Schottky diagrams for pure MoO_3 and V_2O_5 (respectively). Thus, the *n*-type semiconductivity character of the binary MoVO oxide is provided by its molybdenum content (since MoO_3 is a *n*-type semiconductor), while the *p*-type semiconductivity is due to its vanadium content.

Nevertheless, it is also important to mention that V_2O_5 behaves as a *p*-type semiconductor when the oxidation state of vanadium is lower than 4.6, being V^{4+} the main surface vanadium species [44]. However, according to the XPS results obtained for our MoVO catalysts, the surface oxidation state is 4.25 and 4.50 for samples treated at 400 and 500 °C, respectively. In this case, the main donor species responsible for the *n*-type semiconductivity in the binary MoVO oxide [44,45,64,66] are oxygen vacancies which, following Kröger-Vink notation, can be written as V_O^X in their neutral form and as $V_O^{\bullet\bullet}$ in their double-ionized state. On the other hand, the main acceptor species responsible for the *p*-type semiconductivity in the binary MoVO oxide are cation vacancies [44], V_M^X or $V_M^{''}$ (neutral or ionized vacancy, respectively).

When Te^{4+} is incorporated, the resulting ternary MoVTeO oxide mainly shows *n*-type semiconductivity (Fig. 9). Indeed, the linear region with negative slope, typical for *p*-type semiconductors, is almost absent for the trimetallic catalysts. This result agrees with Wernbacher et al. [44], since they showed that tellurium promoted *n*-type

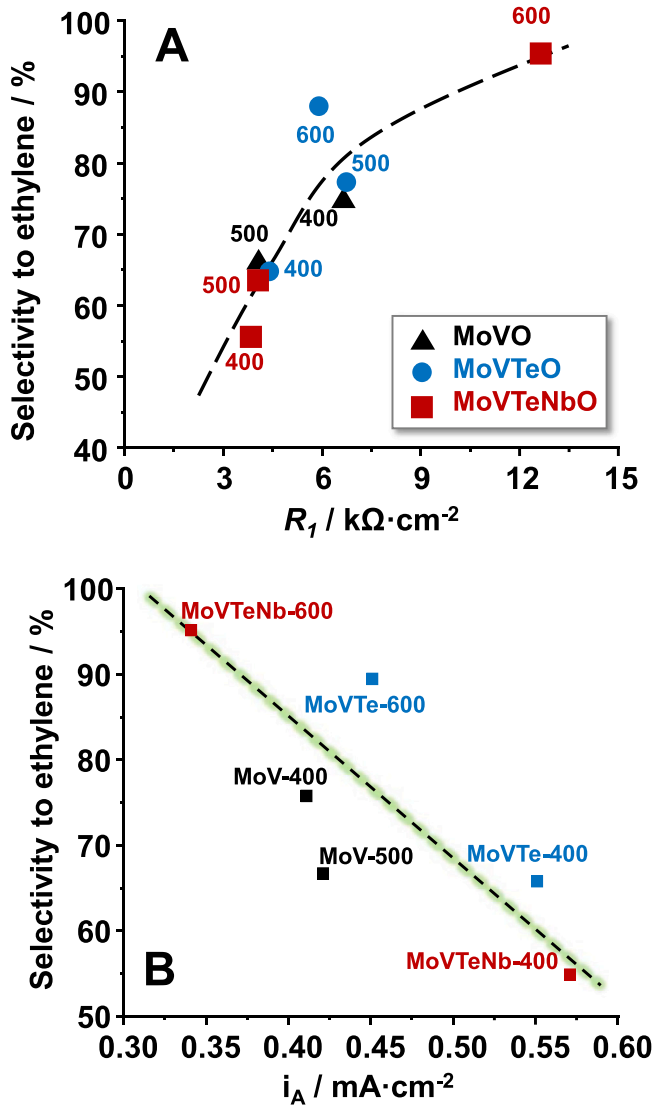

Fig. 8. Relationship between the selectivity to ethylene and the R_1 data (**A**) or the anodic current density, i_A, (**B**) for MoV-, MoVTe- and MoVTeNb-series calcined at 400, 500 and 600 °C. Note: Selectivity at 50 % ethane conversion and a reaction temperature of 390 °C.

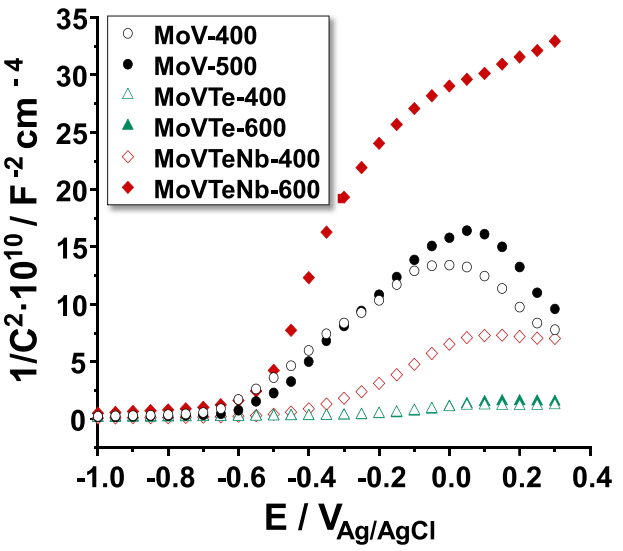

Fig. 9. Mott Schottky plots for representative catalysts of MoV-, MoVTe- and MoVTeNb-series heat-treated at 400 or 600 °C. For comparison it has been also included catalyst **MoV-500**.

semiconductivity in ternary MoVTeO and quaternary MoVTeNbO oxides.

Finally, as stated in [44], the addition of Nb^{5+} clearly favours *n*-type semiconductivity as observed for MoVTeNbO oxides, where the linear region with negative slope is completely eliminated from the Mott-Schottky plots (Fig. 9).

The value of the positive slope in Mott-Schottky plots is inversely related to the density of donor species (oxygen vacancies, as explained above), according to the Mott-Schottky equation. Therefore, the higher the positive slope, the lower the number of oxygen vacancies in the oxide structure. According to the trends shown in Fig. 9, it can be concluded that the MoVTeNbO quaternary oxide heat-treated at 600 °C presents the lowest density of oxygen vacancies, followed by the samples of the MoVO binary oxide (**MoV-500** < **MoV-400**), the quaternary oxide calcined at 400° C and, finally, the MoVTeO oxides (in a same amount).

Furthermore, data of the resistance R_1 presented in Fig. 7d, can be also related to the slope of the Mott-Schottky plots, indicating that the higher the slope, the lower the density of oxygen vacancies and the higher the resistance R_1 to interfacial charge-transfer processes. Consequently, catalysts presenting high slopes in the Mott-Schottky plots should also have higher selectivity to ethylene (fact particularly evident for the **MoVTeNb-600** sample).

In addition, the influence of semiconducting properties on the selectivity to ethylene of these mixed oxides can be explained in terms of defects (vacancies) and oxygen species within the oxide structures. In general, for the ODH reaction, two types of oxygen species have been described in terms of their capacity to affect the selectivity of the reaction: electrophilic oxygen species (O^-), or non-stoichiometric oxygen (NSO), which favour deep oxidation to CO and CO_2, and nucleophilic species (O^{2-}), which favour selective oxidation reactions [1,67–70]. Thus, the relationship between semiconducting properties of the oxide (catalyst) and the prevailing oxygen species within its structure can provide information on its selectivity in ODH reactions.

In oxides showing *p*-type semiconductivity, i.e., the binary MoVO oxides, the taking by a cation vacancy of two electrons from its surroundings results in two positive electron holes and a doubly-ionized cation vacancy ($V_M^{\cdot\cdot}$), according to the following reaction:

$$V_M^X \rightarrow V_M^{\prime\prime} + 2h^{\bullet} \quad (1)$$

These holes can subsequently interact with an oxygen anion located in a regular position within the oxide lattice (O^{2-} or O_O^X using the Kröger-Vink notation), forming an oxygen anion with positive effective charge ($O_O^{\bullet}$), which is equivalent to the electrophilic O^- anion [43,70].

$$O_O^X + h^{\bullet} \rightarrow O_O^{\bullet} \quad (2)$$

Therefore, cation vacancies promote the formation of electrophilic oxygen species which, in turn, lead to low selectivity values to ethylene. This fact would explain the lower selectivity to ethylene obtained for the **MoV-400** sample at high ethane conversion compared to the values obtained for the **MoVTeNb-600** catalyst (Fig. 3), in which the *p*-type semiconductivity is absent.

In oxides showing no (or very little) *p*-type semiconductivity but very low positive slopes in Mott-Schottky plots, i.e., MoVTeO-series (see Fig. 9), oxygen vacancies are the prevailing defects, and their concentration is higher than for the rest of the catalysts. An oxygen vacancy is created from the transfer of an oxygen atom in a normal site of the lattice (O^{2-}/O_O^X) to the gaseous state. Considering the double-ionized form of the vacancy ($V_O^{\bullet\bullet}$), the global reaction can be written as:

$$O_O^X \rightarrow V_O^{\bullet\bullet} + 2e' + \frac{1}{2}O_2(g) \quad (3)$$

Hence, there is competition between nucleophilic oxygen species (O^{2-}/O_O^X), which enhance selectivity to ethylene, and oxygen vacancies, that lead to deep oxidation of the hydrocarbons. Consequently, a high density of these vacancies, such as in the MoVTe-series, may result in lower selectivity to ethylene if compared with the **MoVTeNb-600** sample, whose density of oxygen vacancies is significantly lower (much higher slopes in Mott-Schottky plots). This result agrees with the conclusions obtained by other authors [46]. However, the **MoVTeNb-400** sample, although displaying a higher slope than the corresponding Nb-free **MoVTe-400** catalyst (lower $V_O^{\bullet\bullet}$), presents a lower selectivity to ethylene (Table 2). This fact can be associated with the presence of the M1 phase in the latter (MoVTe-series), that seems to be key in the selective alkane (ethane) activation [9–27]. Accordingly, the electronic structure and semiconducting properties of the different oxides do not directly determine, by themselves, their catalytic performance in terms of their selectivity to ethylene, since other important variables are also involved in the catalytic process (for example, the formation of the M1 phase or the relative surface amount of the different metal cations in the surface). Nevertheless, there is a clear relationship between the semiconducting behaviour of the mixed MoVO, MoVTeO and MoVTeNbO oxides and their catalytic performance (in terms of selectivity). Hence, it can be concluded that, in general, *n*-type semiconductors with low density of oxygen vacancies yield higher selectivity to ethylene in the ethane ODH.

Lastly, Fig. 10 summarizes the results obtained in the present article. Then, it is clear that the formation of the M1 phase, which depends on both the composition and the heat-treatment temperature, is paramount, since its decomposition or its non-formation leads to the lowest olefin production.

However, other factors, especially the amount of surface V^{4+} species, but also the density of oxygen vacancies or the charge transfer resistance, play an essential role. Then, by controlling these other factors further increases in the selectivity towards ethylene can be obtained.

4. Conclusions

In the present article, a comparative study of MoVO, MoVTeO and MoVTeNbO catalysts, heat-treated at 400, 500 or 600 °C in N_2 atmosphere, has been undertaken. Thus, it has been shown that the presence of well-defined orthorhombic M1 crystalline structure is a requirement to achieve optimal catalytic performance in the oxidative dehydrogenation of ethane to ethylene. Interestingly, the formation of the desired M1 phase takes place at different activation temperatures depending on the composition of the catalyst. Then, the M1 phase begins to decompose at temperatures over 400 °C for MoVO catalysts. However, in the case of MoVTe-series, the formation of M1 is optimized in the 400–600 °C activation temperatures range. For MoVTeNb-series, on the contrary, the M1 phase begins to be formed at activation temperatures over 500 °C and it is optimized in the 550–600 °C temperature range. Consequently, the most selective catalysts are those that present the M1 phase with its highest purity, the optimal activation temperature being different depending on the composition.

On the other hand, a clear correlation between the concentration of surface V^{4+} species and the selectivity to ethylene has been observed regardless of the bulk chemical composition and the activation temperature of the sample. Then, a partially reduced surface seems to be required to optimize the catalytic performance.

Additionally, a completely novel electrochemical study has been undertaken on these catalysts. Thus, Electrochemical Impedance Spectroscopy (EIS) studies showed that the higher the charge transfer resistances at the interfacial active parts of the catalysts, the higher is the selectivity to ethylene. Moreover, Mott-Schottky plots, that evaluate the semiconductor behaviour of the catalysts, demonstrated that selectivity to ethylene in the ethane ODH is enhanced in catalysts with *n*-type semiconductivity, presenting low densities of oxygen vacancies, while higher current densities (calculated from cyclic voltammetries) are related, nevertheless, to total oxidation reactions, thus decreasing the selectivity to ethylene specially at high ethane conversion values.

The formulation of the optimal catalysts requires the presence of Nb, although this element is not necessary for the formation of the selective orthorhombic M1 phase. Interestingly, the presence of Nb favours higher thermal stability. Conversely, at low heat-treatments temperatures, it hinders the formation of the orthorhombic phase. Moreover, when the M1 phase is formed in the quaternary catalysts (**MoVTeNb-600**), the presence on the surface of V^{4+} species is maximized. Additionally, it has been reported that the presence of Nb atoms in the M1 phase leads to an enhanced selectivity to ethylene because of the surprisingly low acidity of these catalysts when Nb^{5+} is included in its composition [30]. On the other hand, M1 phase catalysts with acid character present a higher deep oxidation of the olefin (i.e., MoVTe- or MoVSb-based catalysts [32]). Then, the presence of Nb^{5+} in Mo-V-Te-Nb-O M1 oxide minimizes the overoxidation of the olefin by the decrease in the density of acid sites , being essential to achieve high yields to ethylene, as it was previously

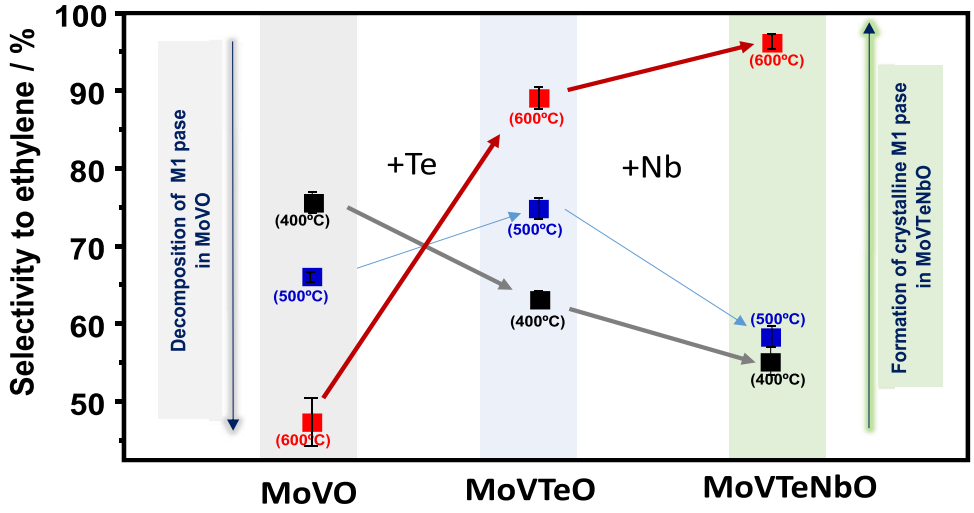

Fig. 10. Variation of selectivity to ethylene at an ethane conversion of 50 % for MoVO, MoVTeO and MoVTeNbO catalysts heat-treated at 400, 500 or 600 °C. Note: catalysts presenting M1 phase, except **MoV-600** (Mo_5O_{14}-based crystalline phase), and **MoVTeNb-400** and **MoVTeNb-500** (pseudocrystalline phase). Black bars correspond to error bars.

reported for the selective propane oxidation to acrylic acid [13,16,30].

Therefore, all together the M1 phase, the specific composition of Nb-containing materials, and the catalyst activation temperature of ca. 600 °C (as occurs in sample **MoVTeNb-600**) favour and are key factors for a higher stabilization of V^{4+} sites with the presence of an optimal V^{4+}/V^{5+} ratio on the surface of the catalyst. Then, and as a consequence of the optimized amount of surface V^{4+} species, other factors such as the density of oxygen vacancies and the charge transfer resistance may also play an important role in the catalytic performance. Thus, by controlling these other factors further increases in the selectivity towards ethylene have been obtained.

CRediT authorship contribution statement

Agustín de Arriba: Investigation, Discussing, Writing – review & editing. **Ginebra Sánchez:** Investigation, Discussing, Writing – review & editing. **Rita Sánchez-Tovar:** Investigation, Discussing, Writing – review & editing. **Patricia Concepción:** Investigation, Discussing, Writing – review & editing. **Ramón Fernández-Domene:** Investigation, Discussing, Writing – review & editing. **Benjamín Solsona:** Supervision, Conceptualization, Validation, Writing – review & editing, Funding. **José M. López Nieto:** Supervision, Conceptualization, Writing – review & editing, Funding.

Declaration of Competing Interest

The authors declare that they have no known competing financial interests or personal relationships that could have appeared to influence the work reported in this paper.

Data Availability

Data will be made available on request.

Acknowledgement

The funding received from the Ministerio de Ciencia e Innovación of Spain, MINECO/FEDER (Projects: PID2021-126235OB-C31, PID2021-126235OB-C33, TED2021-130756B-C32 and TED2021-129555B-I00), for this study is acknowledged. A.A. acknowledges Severo Ochoa Excellence Program for his fellowship (BES-2017-080329).

Appendix A. Supporting information

Supplementary data associated with this article can be found in the online version at doi:10.1016/j.cattod.2023.114122.

References

[1] S. Najari, S. Saeidi, P. Concepcion, D.D. Dionysiou, S.K. Bhargava, A.F. Lee, K. Wilson, Oxidative dehydrogenation of ethane: Catalytic and mechanistic aspects and future trends, Chem. Soc. Rev. 50 (2021) 4564–4605.
[2] A.M. Gaffney, J.W. Sims, V.J. Martin, N.V. Duprez, K.J. Louthan, K.L. Roberts, Evaluation and analysis of ethylene production using oxidative dehydrogenation, Catal. Today 369 (2021) 203–209.
[3] J.T. Grant, J.M. Venegas, W.P. McDermott, I. Hermans, Aerobic oxidations of light alkanes over solid metal oxide catalysts, Chem. Rev. 118 (2018) 2769–2815.
[4] C.A. Gärtner, A.C. v anVeen, J.A. Lercher, Oxidative dehydrogenation of ethane: Common principles and mechanistic aspects, ChemCatChem 5 (2013) 3196–3217.
[5] F. Cavani, N. Ballarini, A. Cericola, Oxidative dehydrogenation of ethane and propane: How far from commercial implementation? Catal. Today 127 (2007) 113–131.
[6] J.M. López, Nieto, The selective oxidative activation of light alkanes. From supported vanadia to multicomponent bulk V-containing catalysts, Top. Catal. 41 (2006) 3–15.
[7] G. Grubert, E. Kondratenko, S. Kolf, M. Baerns, P. van Geem, R. Parton, Fundamental insights into the oxidative dehydrogenation of ethane to ethylene over catalytic materials discovered by an evolutionary approach, Catal. Today 81 (2003) 337–345.
[8] A.M. Gaffney, N.V. Duprez, K.J. Louthan, B. Borders, J. Gasque, A. Siegfried, Th. G. Stanford, K.L. Roberts, Y. Alcheikhhamdona, M. Hoorfar, B. Chen, S. Majumdar, H. Murnen, Ethylene production using oxidative dehydrogenation: effects of membrane-based separation technology on process safety & economics, Catal. Today 371 (2021) 11–28.
[9] P. Botella, E. Garcıa-González, A. Dejoz, J.L. Nieto, M. Vázquez, J. González-Calbet, J. Catal. 225 (2004) 428–438.
[10] J.M. López Nieto, P. Botella, P. Concepción, A. Dejoz, M.I. Vázquez, Oxidative dehydrogenation of ethane on Te-containing MoVNbO catalysts, Catal. Today 91–92 (2004) 241–245.
[11] H. Tsuji, Y. Koyasu, Synthesis of MoVNbTe(Sb)Ox composite oxide catalysts via reduction of polyoxometalates in an aqueous medium, J. Am. Chem. Soc. 124 (2002) 5608–5609.
[12] J.M.M. Millet, H. Roussel, A. Pigamo, J.L. Dubois, J.C. Jumas, Characterization of tellurium in MoVTeNbO catalysts for propane oxidation or ammoxidation, Appl. Catal. A- Gen. 232 (2002) 77–92.
[13] P. Botella, J.M. López Nieto, B. Solsona, A. Mifsud, F. Márquez, The preparation, characterization, and catalytic behavior of MoVTeNbO catalysts prepared by hydrothermal synthesis, J. Catal. 209 (2002) 445–455.
[14] D. Vitry, Y. Morikawa, J.L. Dubois, W. Ueda, Mo-V-Te-(Nb)-O mixed metal oxides prepared by hydrothermal synthesis for catalytic selective oxidations of propane and propene to acrylic acid, Appl. Catal. A: Gen. 251 (2003) 411–424.
[15] Z. Han, X. Yi, Q. Xie, R. Li, H. Lin, Y. He, L. Chen, W. Weng, H. Wan, Oxidative dehydrogenation of ethane over MoVTeNbO catalyst prepared by a slurry method, Chin. J. Catal. 26 (2005) 441–442.
[16] J.M. López Nieto, B. Solsona, P. Concepción, F. Ivar, A. Dejoz, M.I. Vázquez, Reaction products and pathways in the selective oxidation of C_2–C_4 alkanes on MoVTeNb mixed oxide catalysts, Catal. Today 157 (2010) 291–296.
[17] T.T. Nguyen, B. Deniau, P. Delichere, J.M.M. Millet, Influence of the content and distribution of vanadium in the M1 phase of the MoVTe(Sb)NbO catalysts on their catalytic properties in light alkanes oxidation, Top. Catal. 57 (2014) 1152–1162.
[18] P. Kube, B. Frank, S. Wrabetz, J. Kröhnert, M. Hävecker, J. Velasco-Vélez, J. Noack, R. Schölgl, A. Trunschke, Functional analysis of catalysts for lower alkane oxidation, ChemCatChem 9 (2017) 573–585.
[19] Y. Zhu, P.V. Sushko, D. Melzer, E. Jensen, L. Kovarik, C. Ophus, M. Sanchez-Sanchez, J.A. Lercher, N.D. Browning, Formation of oxygen radical sites on MoVNbTeOx by cooperative electron redistribution, J. Am. Chem. Soc. 139 (2017) 12342–12345.
[20] D. Melzer, G. Mestl, K. Wanninger, Y. Zhu, N.D. Browning, M. Sánchez-Sánchez, J. A. Lercher, Design and synthesis of highly active MoVTeNb-oxides for ethane oxidative dehydrogenation, Nat. Commun. 10 (2019) 4012.
[21] J.S. Valente, H. Armendáriz-Herrera, R. Quintana-Solórzano, P. Del Ángel, A. Massó, J.M. López Nieto, Chemical, structural, and morphological changes of a MoVTeNb catalyst during oxidative dehydrogenation of ethane, ACS Catal. 4 (2014) 1292–1301.
[22] L. Annamalai, Y. Liu, S. Ezenwa, Y. Dang, S.L. Suib, P. Deshlahra, Influence of tight confinement on selective oxidative dehydrogenation of ethane on MoVTeNb mixed oxides, ACS Catal. 8 (2018) 7051–7067.
[23] A.M. Gaffney, Q. An, W.A. Goddard III, W. Diao, M.V. Glazoff, Toward concurrent engineering of the M1-based catalytic systems for oxidative dehydrogenation (ODH) of alkanes, Top. Catal. 63 (2020) 1667–1681.
[24] T.Y. Kardash, E.V. Lazareva, D.A. Svintsitskiy, A.V. Ishchenko, V.M. Bondareva, R. B. Neder, The evolution of the M1 local structure during preparation of VMoNbTeO catalysts for ethane oxidative dehydrogenation to ethylene, RSC Adv. 8 (2018) 35903–35916.
[25] B. Chu, H. An, X. Chen, Y. Cheng, Phase-pure M1 MoVNbTeOx catalysts with tunable particle size for oxidative dehydrogenation of ethane, Appl. Catal. A- Gen. 524 (2016) 56–65.
[26] R.K. Grasselli, Site isolation and phase cooperation: Two important concepts in selective oxidation catalysis: a retrospective, Catal. Today 238 (2014) 10–27.
[27] A. de Arriba, B. Solsona, A.M. Dejoz, P. Concepción, N. Homs, P. Ramirez, de la Piscina, J.M. López Nieto, Evolution of the optimal catalytic systems for the oxidative dehydrogenation of ethane: The role of adsorption in the catalytic performance, J. Catal. 408 (2022) 388–400.
[28] X. Tu, M. Niwa, A. Arano, Y. Kimata, E. Okazaki, S. Nomura, Controlled silylation of MoVTeNb mixed oxide catalyst for the selective oxidation of propane to acrylic acid, Appl. Catal. A- Gen. 549 (2018) 152–160.
[29] B. Chu, L. Truter, T.A. Nijhuis, Y. Cheng, Performance of phase-pure M1 MoVNbTeOx catalysts by hydrothermal synthesis with different post-treatments for the oxidative dehydrogenation of ethane, Appl. Catal. A- Gen. 498 (2015) 99–106.
[30] Th.Th Nguyen, B. Deniau, M. Baca, J.-M.M. Millet, Influence of Nb content on the structure, cationic and valence distribution and catalytic properties of MoVTe(Sb) NbO M1 phase used as catalysts for the oxidation of light alkanes, Top. Catal. 59 (2016) 1496–1505.
[31] W. Ueda, K. Oshihara, Selective oxidation of light alkanes over hydrothermally synthesized Mo-V-M-O (M=Al, Ga, Bi, Sb, and Te) oxide catalysts, Appl. Catal. A-Gen. 200 (2000) 135–143.
[32] P. Botella, A. Dejoz, M.C. Abelló, M.I. Vázquez, L. Arrúa, J.M. López, Nieto, Selective oxidation of ethane: developing an orthorhombic phase in Mo–V–X (X= Nb, Sb, Te) mixed oxides, Catal. Today 142 (2009) 272–277.
[33] M. Aouine, T. Epicier, J.-M.M. Millet, In situ environmental STEM study of the MoVTe oxide M1 phase catalysts for ethane oxidative dehydrogenation, ACS Catal. 6 (2016) 4775–4781.
[34] D. Melzer, G. Mestl, K. Wanninger, A. Jentys, M. Sanchez-Sanchez, J.A. Lercher, On the promoting effects of Te and Nb in the activity and selectivity of M1 MoV-oxides for ethane oxidative dehydrogenation, Top. Catal. 63 (2020) 1754–1764.
[35] T. Konya, T. Katou, T. Murayama, S. Ishikawa, M. Sadakane, D. Buttrey, W. Ueda, An orthorhombic Mo_3VOx catalyst most active for oxidative dehydrogenation of

ethane among related complex metal oxides, Catal. Sci. Technol. 3 (2013) 380–387.
[36] S. Ishikawa, X. Yi, T. Murayama, W. Ueda, Heptagonal channel micropore of orthorhombic Mo_3VOx as catalysis field for the selective oxidation of ethane, Appl. Catal. A: Gen. 474 (2014) 10–17.
[37] Sadakane, K. Kodato, N. Yasuda, S. Ishikawa, W. Ueda, Thermal behavior, crystal structure, and solid-state transformation of orthorhombic Mo–V oxide under nitrogen flow or in air, ACS Omega 4 (2019) 13165–13171.
[38] R. Obunai, K. Tamura, I. Ogino, Sh.R. Mukai, W. Ueda, Mo–V–O nanocrystals synthesized in the confined space of a mesoporous carbon, Appl. Catal. A Gen. 624 (2021), 118294.
[39] N. Watanabe, W. Ueda, Comparative study on the catalytic performance of single-phase Mo−V−O-based metal oxide catalysts in propane ammoxidation to acrylonitrile, Ind. Eng. Chem. Res. 45 (2006) 607–614.
[40] D. Vitry, Y. Morikawa, J.L. Dubois, W. Ueda, Propane selective oxidation over monophasic Mo–V–Te–O catalysts prepared by hydrothermal synthesis, Top. Catal. 23 (2003) 47–53.
[41] V. Guliants, R. Bhandari, J.N. Al-Saeedi, V.K. Vasudevan, R.S. Soman, O. Guerrero-Pérez, M.A. Bañares, Bulk mixed Mo–V–Te–O catalysts for propane oxidation to acrylic acid, Appl. Catal. A-Gen. 274 (2004) 123–132.
[42] P. Concepción, S. Hernández, J.M. López Nieto, On the nature of active sites in MoVTeO and MoVTeNbO catalysts: The influence of catalyst activation temperature, Appl. Catal. A. -Gen. 391 (2011) 92–101.
[43] J.M.M. Millet, Mechanism of first hydrogen abstraction from light alkanes on oxide catalysts, Top. Catal. 38 (2006) 83–92.
[44] A.M. Wernbacher, P. Kube, M. Hävecker, R. Schlögl, A. Trunschke, Electronic and dielectric propreties of MoV-oxide (M1 Phase) under alkane oxidation conditions, J. Phys. Chem. C 123 (2019) 13269–13282.
[45] C. Heine, M. Hävecker, A. Trunschke, R. Schlögl, M. Eichelbaum, The impact of steam on the electronic structure of the selective propane oxidation catalyst MoVTeNb oxide (orthorhombic M1 phase), Phys. Chem. Chem. Phys. 17 (2015) 8983–8993.
[46] M. Caldararu, M. Scurtu, C. Hornoiu, C. Munteanu, T. Blasco, J.M. López Nieto, Electrical conductivity of a MoVTeNbO catalyst in propene oxidation measured in operando conditions, Catal. Today 155 (2010) 311–318.
[47] K. Amakawa, Yury V. Kolen'ko, A. Villa, M.E. Schuster, L.-I. Csepei, G. Weinberg, S. Wrabetz, R.N. d'Alnoncourt, F. Girgsdies, L. Prati, R. Schlögl, Annette Trunschke, Multifunctionality of crystalline MoV(TeNb) M1 oxide catalysts in selective oxidation of propane and benzyl alcohol, ACS Catal. 3 (2013) 1103–1113.
[48] H. Knözinger, H.Jezlorowski Raman, spectra of molybdenum oxide supported on the surface of aluminas, J. Phys. Chem. 82 (1978) 2002–2005.
[49] X.-J. Yang, R.M. Feng, W.-J. Ji, Ch-T. Au, Characterization and evaluation of MoVTeNb mixed metal oxide catalysts fabricated via hydrothermal process with ultrasonic pretreatment for propane partial oxidation, J. Catal. 253 (2008) 57–65.
[50] P. DeSanto Jr., D.J. Buttrey, R.K. Grasselli, C.G. Lugmair, A.F. Volpe, B.H. Toby, Th. Vogt, Structural characterization of the orthorhombic phase M1 in MoVNbTeO propane ammoxidation catalyst, Top. Catal. 23 (2003) 23–38.
[51] A. Celaya Sanfiz, T.W. Hansen, A. Sakthivel, A. Trunschke, R. Schlögl, A. Knoester, H.H. Brongersma, M.H. Looi, S.B.A. Hamid, How important is the (001) plane of M1 for selective oxidation of propane to acrylic acid? J. Catal. 258 (2008) 35–43.
[52] L. Annamalai, S. Ezenwa, Y. Dang, H. Tan, S.L. Suib, P. Deshlahra, Comparison of structural and catalytic properties of monometallic Mo and V oxides and M1 phase mixed oxides for oxidative dehydrogenation, Catal. Today 368 (2021) 28–45.
[53] Y.V. Kolen'Ko, W. Zhang, R.N. D'Alnoncourt, F. Girgsdies, T.W. Hansen, T. Wolfram, R. Schlögl, A. Trunschke, Synthesis of MoVTeNb oxide catalysts with tunable particle dimensions, ChemCatChem 3 (2011) 1597–1606.
[54] R. Schlögl, Active sites for propane oxidation: some generic considerations, Top. Catal. 54 (2011) 627–638.
[55] P. Botella, J.M. López Nieto, B. Solsona, A. Mifsud, F. Márquez, The preparation, characterization, and catalytic behavior of MoVTeNbO catalysts prepared by hydrothermal synthesis, J. Catal. 209 (2002) 445–455.
[56] A. Trunschke, J. Noack, S. Trojanov, F. Girgsdies, T. Lunkenbein, V. Pfeifer, M. Hävecker, P. Kube, C. Sprung, F. Rosowski, R. Schlögl, The impact of the bulk structure on surface dynamics of complex Mo–V-based oxide catalysts, ACS Catal. 7 (2017) 3061–3071.
[57] A. Celaya Sanfiz, T.W. Hansen, F. Girgsdies, O. Timpe, E. Rodel, T. Ressler, A. Trunschke, R. Schlögl, Preparation of phase-pure M1 MoVTeNb oxide catalysts by hydrothermal synthesis—influence of reaction parameters on structure and morphology, Top. Catal. 50 (2008) 19–32.
[58] D.A. Svintsitskiy, T.Yu Kardash, E.V. Lazareva, V.M. Bondareva, X-ray-induced transformations on the surface of MoVNbTe mixed oxide catalyst: an XPS study, Appl. Surf. Sci. 535 (2021), 147676.
[59] B. Grzybowska-Świerkosz, Active centres on vanadia-based catalysts for selective oxidation of hydrocarbons, Appl. Catal. A-Gen. 157 (1997) 409–422.
[60] J.M. López Nieto, The selective oxidative activation of light alkanes. From supported vanadia to multicomponent bulk V-containing catalysts, Top. Catal. 41 (2006) 3–15.
[61] R.K. Grasselli, A.F. Volpe Jr., Catalytic consequences of a revised distribution of key elements at the active centers of the M1 phase of the MoVNbTeOx system, Top. Catal. 57 (2014) 1124–1137.
[62] X. Li, D.J. Buttrey, D.A. Blom, Th. Vogt, Improvement of the structural model for the M1 Phase Mo–V–Nb–Te–O propane (amm)oxidation catalyst), Top. Catal. 54 (2011) 614–626.
[63] R.M. Fernández-Domene, R. Sánchez-Tovar, B. Lucas-granados, M.J. Muñoz-Portero, J. García-Antón, Elimination of pesticide atrazine by photoelectrocatalysis using a photoanode based on WO_3 nanosheets, Chem. Eng. J. 350 (2018) 1114–1124.
[64] I.A. de Castro, R.S. Datta, J.Z. Ou, A. Castellanos-Gomez, S. Sriram, T. Daeneke, K. Kalantar-zadeh, Molybdenum oxides – from fundamentals to functionality, Adv. Mater. 29 (2017) 1–31.
[65] R.M. Fernández-Domene, G. Roselló-Márquez, R. Sánchez-Tovar, B. Lucas-Granados, J. García-Antón, Photoelectrochemical removal of chlorfenvinphos by using WO3 nanorods: influence of annealing temperature and operation pH, Sep. Purif. Technol. 212 (2019) 458–464.
[66] Y. Zhu, Y. Yao, Z. Luo, C. Pan, J. Yang, Y. Fang, H. Deng, C. Liu, Q. Tan, F. Liu, Y. Guo, Nanostructured MoO_3 for efficient energy and environmental catalysis, Molecules 25 (2020) 1–26.
[67] E. Heracleous, A.A. Lemonidou, Ni-Nb-O mixed oxides as highly active and selective catalysts for ethene production via ethane oxidative dehydrogenation. Part I: Characterization and catalytic performance, J. Catal. 237 (2006) 162–174.
[68] X. Zhao, M.D. Susman, J.D. Rimer, P. Bollini, Tuning selectivity in nickel oxide-catalyzed oxidative dehydrogenation of ethane through control over non-stoichiometric oxygen density, Catal. Sci. Technol. 11 (2021) 531–541.
[69] D.M. Gómez, V.V. Galvita, J.M. Gatica, H. Vidal, G.B. Marin, TAP study of toluene total oxidation over a Co_3O_4/La-CeO_2 catalyst with an application as a washcoat of cordierite honeycomb monoliths, Phys. Chem. Chem. Phys. 16 (2014) 11447–11455.
[70] I. Popescu, Z. Skoufa, E. Heracleous, A. Lemonidou, I.C. Marcu, A study by electrical conductivity measurements of the semiconductive and redox properties of Nb-doped NiO catalysts in correlation with the oxidative dehydrogenation of ethane, Phys. Chem. Chem. Phys. 17 (2015) 8138–8147.